

# Dissepiments, density bands and signatures of thermal stress in *Porites* skeletons

Thomas M. DeCarlo<sup>1,3</sup> · Anne L. Cohen<sup>2</sup>

Received: 26 October 2016 / Accepted: 5 March 2017  
© Springer-Verlag Berlin Heidelberg 2017

**Abstract** The skeletons of many reef-building corals are accreted with rhythmic structural patterns that serve as valuable sclerochronometers. Annual high- and low-density band couplets, visible in X-radiographs or computed tomography scans, are used to construct age models for paleoclimate reconstructions and to track variability in coral growth over time. In some corals, discrete, anomalously high-density bands, called “stress bands,” preserve information about coral bleaching. However, the mechanisms underlying the formation of coral skeletal density banding remain unclear. Dissepiments—thin, horizontal sheets of calcium carbonate accreted by the coral to support the living polyp—play a key role in the upward growth of the colony. Here, we first conducted a vital staining experiment to test whether dissepiments were accreted with lunar periodicity in *Porites* coral skeleton, as previously hypothesized. Over 6, 15, and 21 months, dissepiments consistently formed in a 1:1 ratio to the number of full moons elapsed over each study period. We measured

dissepiment spacing to reconstruct multiple years of monthly skeletal extension rates in two *Porites* colonies from Palmyra Atoll and in another from Palau that bleached in 1998 under anomalously high sea temperatures. Spacing between successive dissepiments exhibited strong seasonality in corals containing annual density bands, with narrow (wide) spacing associated with high (low) density, respectively. A high-density “stress band” accreted during the 1998 bleaching event was associated with anomalously low dissepiment spacing and missed dissepiments, implying that thermal stress disrupts skeletal extension. Further, uranium/calcium ratios increased within stress bands, indicating a reduction in the carbonate ion concentration of the coral’s calcifying fluid under stress. Our study verifies the lunar periodicity of dissepiments, provides a mechanistic basis for the formation of annual density bands in *Porites*, and reveals the underlying cause of high-density stress bands.

Communicated by Biology Editor Dr. Mark R. Patterson

**Electronic supplementary material** The online version of this article (doi:10.1007/s00338-017-1566-9) contains supplementary material, which is available to authorized users.

✉ Thomas M. DeCarlo  
thomas.decarlo@uwa.edu.au

<sup>1</sup> Massachusetts Institute of Technology/Woods Hole Oceanographic Institution Joint Program in Oceanography and Applied Ocean Science and Engineering, Woods Hole, MA 02543, USA

<sup>2</sup> Woods Hole Oceanographic Institution, Woods Hole, MA 02543, USA

<sup>3</sup> Present Address: School of Earth and Environment, The University of Western Australia, Crawley, Australia

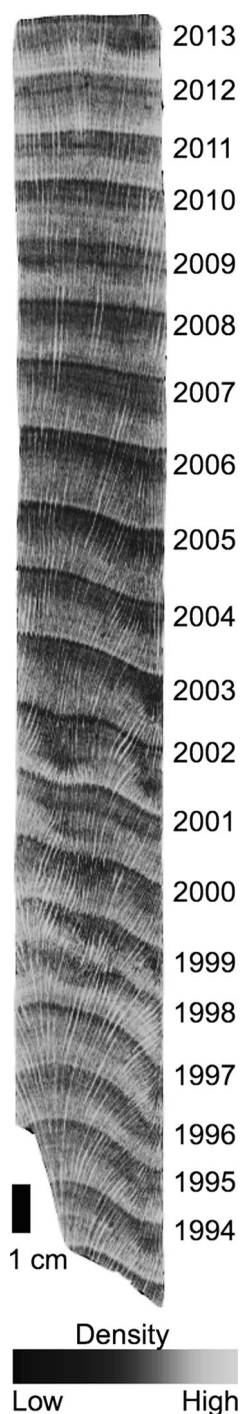
**Keywords** Coral · Calcification · Density banding · Sclerochronology · Stress bands · Bleaching

## Introduction

The history of the tropical oceans is archived in the calcium carbonate (CaCO<sub>3</sub>) skeletons of reef-building corals. Some corals live for a millennium and build massive 10-m-tall colonies (Soong et al. 1999) but, despite their size, only thin layers (2 cm or less) of living polyps envelop them. Below this veneer of life, buried within the interior of the colony, is the skeleton constructed over the lifespan of the coral. Rhythmic patterns in the skeleton correspond to specific periods of time, making corals valuable “sclerochronometers,” analogous to tree rings used in

dendrochronology (Buddemeier 1974; Hudson et al. 1976). Scleractinian corals accrete skeleton with different  $\text{CaCO}_3$  crystal morphologies between day and night (Barnes 1970; Gladfelter 1983; Cohen et al. 2001; Cohen and McConnaughey 2003; Shirai et al. 2012) and with different densities between summer and winter (Fig. 1) (Knutson 1972; Buddemeier et al. 1974; Highsmith 1979; Barnes and Lough 1993; Dodge et al. 1993). Skeletal growth patterns have been exploited to reconstruct Earth's astronomic and

**Fig. 1** Density bands visible in computed tomography scan of a *Porites* skeleton collected on Dongsha Atoll, Taiwan. Dark/light shading represents relatively low/high density. The image contrast was adjusted for clarity using the histogram equalization function in ImageJ



climatic history. For example, Wells (1963) combined circadian ( $\sim\text{d}^{-1}$ ) and annual ( $\sim\text{yr}^{-1}$ ) growth ridges in fossil solitary corals to track changes in day length over millions of years. Annual density bands are commonly used to assign calendar dates to geochemical climate proxies measured in the skeleton, such as  $\text{Sr}/\text{Ca}$  or  $\delta^{18}\text{O}$  (Weber and Woodhead 1972; Smith et al. 1979). In some cases, the accuracy of these dates—called “age models”—has been independently verified based on the presence of radioactive isotopes in bands corresponding to mid-twentieth century nuclear tests (Knutson et al. 1972) and recently based on U–Th dating (Thompson et al. 2003; Cobb et al. 2003).

In addition to their chronometric value, density bands provide insight into the sensitivity of corals to climate change. As anthropogenic  $\text{CO}_2$  emissions drive warming and acidification of the oceans, decreases in calcification rates and increases in the frequency of bleaching events are among the impacts projected for corals (Hoegh-Guldberg et al. 2007). Yet direct observations of these impacts are limited due to the difficulty of regularly monitoring reefs, especially those in remote locations. In lieu of direct observations, studies of the response of corals to climate change often rely on retrospective analyses of coral growth rates and bleaching histories, both of which have been interpreted from skeletal banding patterns (Dodge and Vaisnys 1975; Lough and Barnes 1992; Carilli et al. 2009a,b; Cantin et al. 2010; Castillo et al. 2012; Barkley and Cohen 2016). Coral growth histories are based on variations in the distance between successive annual density bands (Knutson et al. 1972), and observations of the sensitivity of growth to temperature have been exploited in the reconstruction of paleotemperature records (Saenger et al. 2009). Anomalously high-density bands have been linked to known coral reef bleaching events (Hudson 1981a, b; Dodge et al. 1993; Smithers and Woodroffe 2001; Mendes and Woodley 2002; Carilli et al. 2009a, b; Cantin and Lough 2014; Mallela et al. 2015; Barkley and Cohen 2016), prompting the term “stress bands” and their use as proxies for past bleaching (Carilli et al. 2009a, b; Barkley and Cohen 2016).

Despite the widespread application of annual density bands, and recently of stress bands, it is not entirely understood why, or how, corals accrete bands of varying density (Helmle and Dodge 2011). Published studies on the origins of coral banding generally agree that the rates of upward skeletal extension and/or the accretion of skeletal elements with variable thickness are sensitive to some environmental forcing(s) and this ultimately produces bands of variable density (e.g., Highsmith 1979; Barnes and Lough 1993; Dodge et al. 1993; reviewed in Helmle and Dodge 2011). Temperature and light are often cited as potential environmental drivers of calcification, yet they do

not explain all the variability in density-banding patterns (Helmle and Dodge 2011). Barnes and Lough (1993) and Taylor et al. (1993), investigating *Porites*, and Dodge et al. (1993), investigating *Orbicella*, suggested that annual density banding could arise from seasonal changes in calcification rate, whereby skeletal elements of variable thickness are deposited over the course of a year in response to annual temperature or light cycles. Comparing growth rates to density-banding patterns on sub-annual timescales is one way to test these hypotheses (Barnes and Lough 1993). However, without a proven sub-annual sclerochronometer, one that is independent of density bands, it has been difficult to measure seasonal variations in growth for comparison to skeletal density.

Additional chronometers, recording frequencies between circadian and annual, may be preserved within coral skeletons. Buddemeier (1974) observed fine density bands superposed on the more conspicuous annual bands and speculated that these fine bands may form with lunar rhythm (every  $\sim 29.5$  d, or  $\sim 12.4$  yr<sup>-1</sup>). Barnes and Lough (1989, 1993) suggested that the fine sub-annual bands are related to dissepiments, thin (tens of micrometers) sheets of skeleton oriented perpendicular to the main axis of upward growth. Living coral polyps rest atop the most recent dissepiment (Sorauf 1970), and periodically form a new one, like a ladder rung, to climb higher as they extend the skeleton (Fig. 2). Relic, outgrown dissepiments are buried in the skeleton below, preserving the history of the coral polyps' ascent (cf. Fig. 2 in Barnes and Lough 1992 and Figs. 2, 3 here). At the very outset, Buddemeier (1974) suggested that his lunar rhythm hypothesis should be tested with a vital staining experiment. Yet, to our knowledge, such a test has not been successfully performed. Buddemeier and Kinzie (1975) attempted to test dissepiment lunar rhythm by repeatedly staining the skeletons of living corals in successive months. However, they were unable to reliably identify the skeleton formed over one month because some stain lines were either missing or merged. Using a different approach, Barnes and Lough (1993) compared dissepiments to presumed annual density bands and found in some cases 12, but sometimes as few as 3–6, dissepiments per year. They concluded that their observed upper limit of 12 dissepiments between annual bands was consistent with lunar rhythm, but limitations in their method of identifying dissepiments and uncertainty in defining precisely one calendar year from density banding (Lough and Barnes 1990) precluded a definitive test of the lunar rhythm hypothesis. Thus, the question remains whether corals form dissepiments with regular periodicity, and if so, what the characteristic timescale is.

Here, we first test the lunar rhythm hypothesis by tracking dissepiment formation over precisely known

periods of time and then use dissepiments to investigate the formation of skeletal density bands. Like Buddemeier and Kinzie (1975), we tracked skeletal accretion with vital staining of the skeletons of living *Porites* spp. colonies, but we followed Barnes and Lough (1993) in recording dissepiments over  $>1$  yr, rather than successive months. Within the framework of our dissepiment frequency results, we examine the role of monthly changes in skeletal extension rate in the formation of both annual density bands and anomalously high-density “stress” bands.

## Materials and methods

### Lunar rhythm

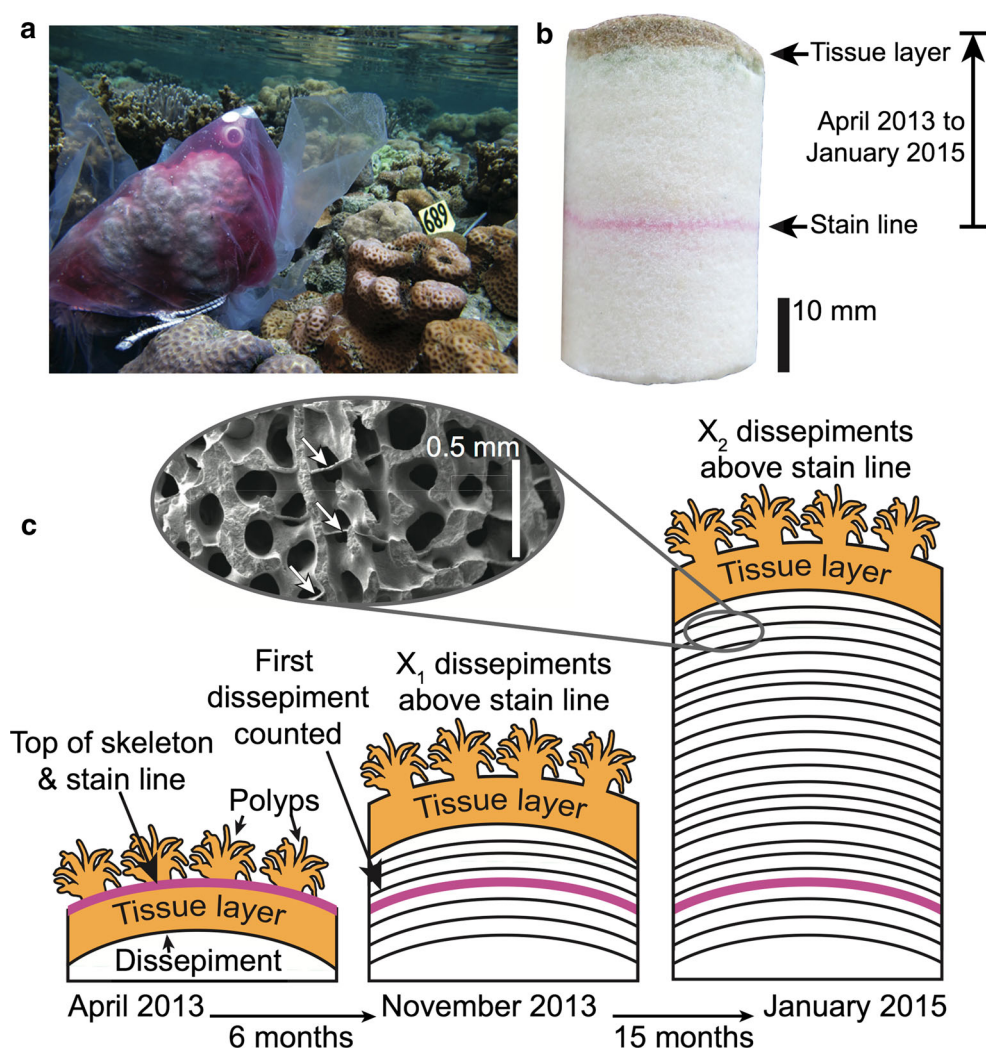
#### *Study design to test dissepiment frequency*

To test for lunar periodicity of dissepiment formation, we placed time markers in the skeletons of living *Porites* colonies using vital stain. Critically, however, the stain is incorporated mainly at the outermost growing tip of the skeleton (Barnes and Lough 1993), whereas dissepiments are located at the base of the tissue layer, which can be anywhere from 2 to 12 mm thick in *Porites* (Figs. 2, 3c). Consequently, several dissepiments may form after staining has occurred but appear below the stain line when the stained coral is examined (Fig. 2). To address this issue, we sampled the skeletons of each colony twice, 6 and 21 months after staining, and tracked the number of dissepiments formed between the first and second sampling (Fig. 2c).

#### *Coral staining and coring*

During 27–28 April 2013, twenty *Porites* colonies living at 1–5 m depths in the Republic of Palau were stained with alizarin red-S dye. Alizarin is taken up by the coral polyp almost immediately and deposited into the growing skeleton. Thus, alizarin has long been used to mark specific dates in the skeleton of living corals (Barnes 1970; Buddemeier and Kinzie 1975; Hudson 1981a; Barnes and Lough 1993; Mendes and Woodley 2002). We stained 20 colonies, 10 each in Nikko Bay (7.323°N, 134.494°E) and on Uchelbeluu reef (7.267°N, 134.521°E). Nikko Bay is a back reef/lagoonal environment with relatively low water flow, low light due to shading from limestone cliffs, and low pH, compared to the barrier reef site, Uchelbeluu (Shamberger et al. 2014; Barkley et al. 2015). Each colony was covered with a translucent plastic bag tied around the base of the colony. A scintillation vial containing 20 mL of 2 g L<sup>-1</sup> alizarin solution was opened inside of each bag (Fig. 2a). We estimate that this procedure resulted in an

**Fig. 2** **a** Alizarin dye released inside a bag covering a live *Porites* coral on April 27, 2013. **b** A stained skeleton core collected in January 2015. The pink line in the skeleton marks the location of the skeletal surface at the time of staining. **c** Schematic of study design.  $X_1$  marks the initial time point in November 2013.  $X_2$  marks the second time point in January 2015. *Inset* shows scanning electron microscope image of *Porites* skeleton with three visible dissepiments (white arrows)



initial concentration of alizarin inside each bag of approximately  $3\text{--}5\text{ mg kg}^{-1}$  and diluted the seawater by  $<1\%$ . Experimental evidence suggests that this concentration of alizarin is unlikely to impact calcification (Holcomb et al. 2013). After 4–6 h, the bags were removed.

Ten of the 20 colonies initially stained were located during subsequent sampling expeditions but we were unable to locate the ten remaining colonies, likely because either the tags or the colonies themselves were dislodged during storms. The skeletons of nine of the 20 stained colonies were located and sampled twice, on 4 November 2013 and 9–10 January 2015, to measure the number of dissepiments formed over time. A core 3.5 cm in diameter and 5–7 cm in length was removed from each colony during each sampling period using an underwater pneumatic drill (Fig. 2b). Core holes were capped with cement plugs, and underwater epoxy was applied to hold the plugs in place. A tenth coral (tag # 682) was located and sampled in Nikko Bay only in January 2015. In colony 682 and in another colony sampled in November 2013 (tag # 689), a

faint secondary stain line was visible 3–5 mm below the primary stain line (Electronic supplementary material, ESM, Fig. S1). These secondary stain lines were not present in all cores, potentially reflecting differences in calcification (rate and distribution within the calyx), or that dye leaked out of some bags during the course of the experiment. Since tissue thickness of our corals is likewise 3–5 mm, and *Porites* calcify throughout their tissue layer (Barnes and Lough 1993), we interpret the secondary stain lines as marking the base of the tissue layer in these two colonies at the time of staining. Therefore, we can evaluate the number of dissepiments formed by these colonies since the initial staining in April 2013.

#### *Coral density, extension, and calcification*

Each core was scanned with computed tomography (CT) using the Siemens Volume Zoom Spiral CT scanner at Woods Hole Oceanographic Institution. Skeletal bulk density ( $\text{g cm}^{-3}$ ) was calculated from calibrated density



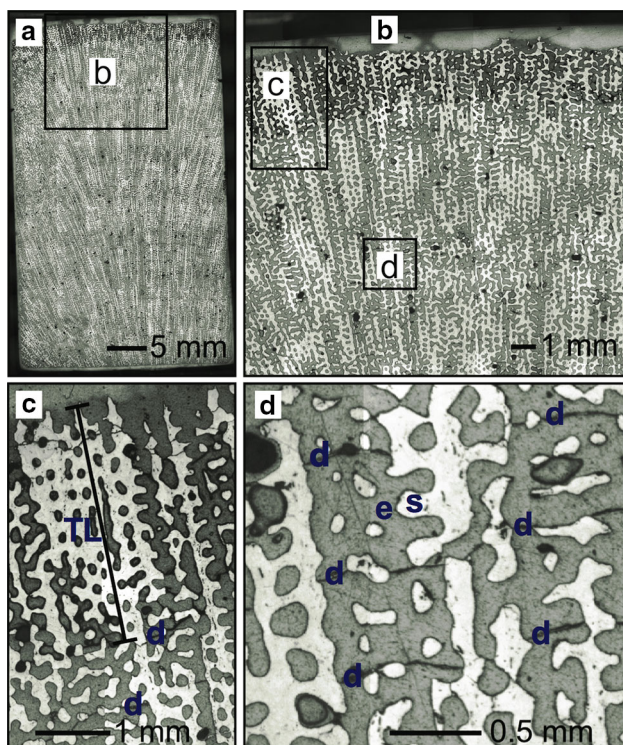


**Fig. 3** **a** Reflected light microscope mosaic of 80 images stitched together to view the entire section cut from the skeleton sample of colony 678. The image contrast was adjusted for clarity using the histogram equalization function in ImageJ. **b–d** Dissepiments in magnified images of the same section as **a**. In **c**, the most recent dissepiment is at the bottom of the tissue layer. In **d**, previous dissepiments preserved in the skeleton are visible as *thin lines*. TL tissue layer, *s* skeleton, *e* epoxy, *d* dissepiment

standards (DeCarlo et al. 2015b) using the software program coralCT (DeCarlo and Cohen 2016). Extension ( $\text{cm yr}^{-1}$ ) was measured as the distance from the top of the stain line to the top of the skeleton, and calcification ( $\text{g cm}^{-2} \text{yr}^{-1}$ ) was calculated as the product of density and extension.

#### Dissepiment mapping

A section approximately 25 mm width by 40 mm height and 3 mm thick was cut from each skeleton sample using a wet diamond wafering blade, sonicated in deionized water for 15 min, and dried overnight in an oven at 50 °C. The sections were then mounted in epoxy on a glass slide and polished (with final grit of 0.25  $\mu\text{m}$ ). A Zeiss Axio Imager 2 microscope with an automated stage was used to collect photomosaics of each section. Images were taken with a 2.5X lens using reflected light. Each photomosaic contained 80–100 images, which were stitched together using Zeiss AxioVision software. Stain lines were visualized using the same procedure, but with transmitted light. The transmitted light photomosaics were superposed on those

collected with reflected light, and the top margins of the stain lines were traced onto the reflected light photomosaics. Dissepiments were clearly visible in the reflected light photomosaics (Fig. 3) and were traced throughout each section to produce dissepiment maps (Fig. 4).

#### Dissepiment counting

We counted the number of dissepiments in each section beginning from the first dissepiment formed above the stain line (Fig. 4). Although the stain lines were accurately mapped onto the reflected light photomosaics, there is potential for uncertainty of one dissepiment count because in some cases it was difficult to identify whether a dissepiment was slightly above or below the top margin of the stain line. Further, since the duplicate cores collected from each colony were spaced 5–10 cm apart, there is potential for our results to reflect slight differences in the stain location or dissepiment patterns across the colony. Bud-demeier and Kinzie (1975) repeatedly stained living *Porites* colonies with alizarin and likewise found uncertainty of one dissepiment with respect to the location of the stain line. Some dissepiments appear as arches, connected to the dissepiment below and not continuous across adjacent

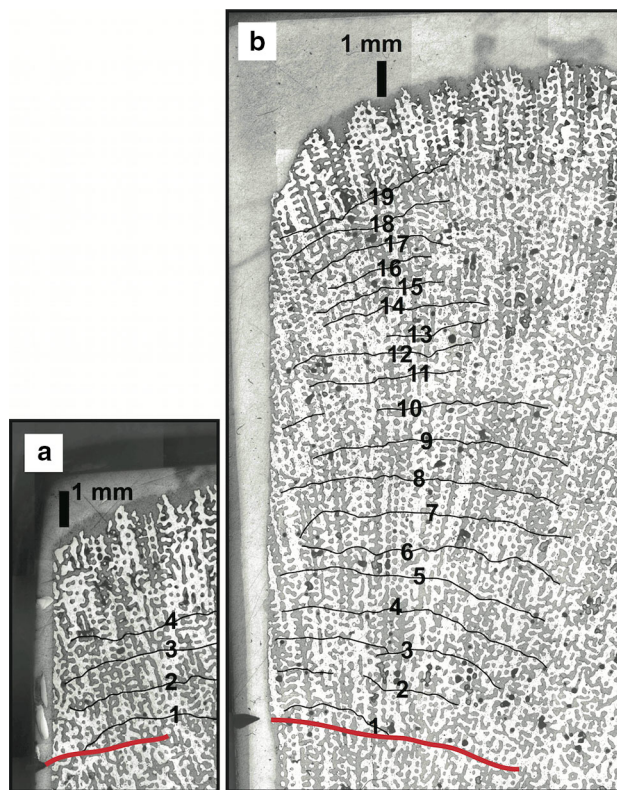


**Fig. 4** Dissepiments mapped from reflected light photomosaic of the skeleton sampled from colony 675 in November 2013 (**a**) and January 2015 (**b**). *Black lines* are traced dissepiments, and the *red line* indicates the April 2013 stain line

corallites (Barnes and Lough 1993 called this “blistering”). As suggested by Barnes and Lough (1993), we counted each blistering as a new dissepiment. Dissepiment maps of each colony are provided in ESM Figs. S2–10.

### Density banding and dissepiment spacing

#### *Dissepiment time series*

To compare the pattern of dissepiments to density banding, we followed the same dissepiment mapping procedure for two *Porites* corals from the southern fore reef of Palmyra Atoll (5.866°N, 162.109°W) in the central Pacific Ocean. These two corals were selected for dissepiment analysis because even though they were collected within 5 m of each other and at the same depth (13 m), one coral has exceptionally clear density banding while the other coral has almost no visible banding pattern. A CT scan of one of these cores (Palmyra colony 03) and geochemical data from both cores are reported in DeCarlo et al. (2016).

An additional coral from Palau was also used for dissepiment spacing measurements. This core was collected from a colony in Airai Bay (7.329°N, 134.557°E) and drilled to a depth of 30 cm into the skeleton. Based on annual density banding, we determined that the skeleton at the bottom of the core was accreted in 1990. We identified an anomalous high-density stress band corresponding to 1998, when mass bleaching was observed in Palau (Bruno et al. 2001). CT data from this core were used in DeCarlo et al. (2015b) and Barkley and Cohen (2016), and geochemical data from this core (discussed below) were presented in DeCarlo et al. (2016).

We used the dissepiment maps of the Palmyra and Airai corals to measure the spacing between consecutive pairs of dissepiments. This spacing, however, is not constant along the axis perpendicular to growth because dissepiments are not completely flat. We measured the average spacing across several adjacent corallites using ImageJ software by measuring the cross-sectional area between two consecutive dissepiments and dividing by the horizontal distance over which the area was measured.

#### *Density banding model*

To evaluate the role of dissepiment spacing in producing density bands, we made a simple model of skeletal growth for the Palmyra 03 colony following Taylor et al. (1993). We set the monthly extension rate equal to the dissepiment spacing and assumed an exponentially decreasing profile of calcification rate (i.e., skeletal thickening) within the 7-cm tissue layer (ESM Fig. S11). In the model, the tissue layer calcification profile was iteratively moved upward each month by a distance equal to the dissepiment spacing.

Next, the calcification rates in relative units were summed for each layer in the skeleton, and the absolute density was calculated by setting the multi-year bulk calcification rate from the model equal to measured value of  $2 \text{ g cm}^{-2} \text{ yr}^{-1}$ . This analysis produced a modeled skeletal density time series that we compared to the density measured from the CT scan using the software coralCT (DeCarlo and Cohen 2016).

## Results

### Lunar rhythm

Between 4 November 2013 and 9–10 January 2015, six corals formed the same number of dissepiments as full moons (15), one coral formed 14 dissepiments, and two formed 16 dissepiments (Table 1). It is possible that the corals that did not form 15 dissepiments represent real deviations from lunar rhythm. As discussed below, dissepiments may be missing during thermal stress and extra dissepiments may form during polyp budding. Nevertheless, all the corals were within measurement uncertainty ( $\pm 1$ ) of 15 dissepiments, and thus, we cannot reject lunar rhythm for any of our samples. Secondary stain lines were visible in two skeletal samples, allowing us to evaluate the number of dissepiments formed since the initial staining. One colony (tag # 689) formed 6 dissepiments between April 2013 and November 2013, and another (tag # 682) formed 21 dissepiments between April 2013 and January 2015, both of which correspond exactly to the number of full moons over the respective time periods. The number of dissepiments formed did not change even though the corals studied represented a wide range of bulk skeletal density ( $1.11\text{--}1.49 \text{ g cm}^{-3}$ ), extension ( $0.73\text{--}1.34 \text{ cm yr}^{-1}$ ), calcification ( $0.89\text{--}1.65 \text{ g cm}^{-2} \text{ yr}^{-1}$ ), and tissue layer thickness ( $2.5\text{--}4.9 \text{ mm}$ ) (Table 1).

One coral (tag # 690) initially appeared to form more than one dissepiment per lunar month between November 2013 and January 2015 (ESM Fig. S10). Within this coral, repeated dissepiment blistering resulted in up to 27 dissepiments above the stain line in January 2015. Dissepiment blistering corresponded to corallite splitting (the result of polyp budding) in this section. If the region of corallite splitting was avoided, 19 dissepiments were counted above the stain line in January 2015 and 3 above the stain line in November 2013, which agreed with the number of full moons elapsed.

### Density banding and dissepiment spacing

We mapped dissepiments from the two Palmyra corals over 4–5 yr of growth. The spacing between consecutive

**Table 1** Coral growth parameters and dissepiment frequency

Coral ID	Site	Density (g cm <sup>-3</sup> )	Extension (cm yr <sup>-1</sup> )	Calcification (g cm <sup>-2</sup> yr <sup>-1</sup> )	Tissue layer (mm)	Dissepiments above stain Nov. 2013	Dissepiments above stain Jan. 2015	Dissepiments formed Nov. 2013 to Jan. 2015
675	Uchelbeluu	1.49	1.11	1.65	2.7	4	19	15
678	Uchelbeluu	1.27	1.05	1.33	3.6	6	22	16
683	Nikko Bay	1.26	0.94	1.18	4.9	1	16	15
684	Nikko Bay	1.25	0.96	1.20	3.3	1	16	15
685	Nikko Bay	1.22	0.73	0.89	2.5	1	16	15
687	Nikko Bay	1.11	1.08	1.20	4.5	5	20	15
688	Nikko Bay	1.22	1.20	1.46	4.6	2	17	15
689	Nikko Bay	1.13	1.34	1.51	4.4	3	17	14
690	Nikko Bay	1.20	1.18	1.18	2.5	3	19	16

dissepiments exhibited a rhythmic seasonal pattern with a period of 12–13 dissepiments ( $p < 0.05$  compared to white noise spectra) in Palmyra colony 03. Conversely, Palmyra colony 02 did not exhibit a regular pattern of dissepiment spacing ( $p > 0.05$  for all frequencies compared to white noise spectra). In addition, the CT scans revealed clear high- and low-density bands in Palmyra 03, but very little density variability in Palmyra 02.

In the coral from Airai Bay, Palau, dissepiment spacing decreased sharply within a stress band corresponding to the year 1998. During 1998, decreases in both the dissepiment spacing and the bulk annual calcification rate were anomalous relative to the preceding 7 yr. Minimum dissepiment spacing in 1998 was 0.6 mm, half that of the 1991–1999 mean of 1.2 mm, and the bulk calcification rate was 1.3 g cm<sup>-2</sup> yr<sup>-1</sup> in 1998 compared to 2.0 g cm<sup>-2</sup> yr<sup>-1</sup> on average between 1991 and 1999. Further, only ten dissepiments were counted between the 1998 and 1999 low-density bands, indicating that dissepiment formation stopped for 2–3 months.

## Discussion

### Lunar rhythm

We conducted a vital staining experiment and found that *Porites* corals accrete new dissepiments with lunar rhythm. Our findings are consistent with previous suggestions that dissepiments are lunar (Buddemeier 1974; Barnes and Lough 1993; Winter and Sammarco 2010); we confirmed these earlier hypotheses by successfully tracking dissepiment formation over precisely known periods exceeding one year.

The coral polyps within each colony must follow a cue to build new dissepiments in synchrony. Dissepiments are continuous across multiple adjacent corallites in perforate

genera such as *Porites* (Fig. 3), and the most recent dissepiment is always located at the base of the entire tissue layer (i.e., there are no gaps in the dissepiment “floor”). These observations can only be explained if polyps across the colony build new dissepiments at about the same time. Our findings strongly suggest that the moon is the cue. Two potential cues linked to the moon are the spring/neap tidal cycle and moonlight. Tides are unlikely to cue dissepiment formation because there are two spring and two neap tides per lunar month, twice the frequency of dissepiment formation. Alternatively, corals may respond to changes in the intensity or spectra of moonlight over the course of a lunar month. Photoreceptors and gene expression in corals are highly sensitive to moonlight spectra (Gorbunov and Falkowski 2002; Sweeney et al. 2011; Kaniewska et al. 2015), and it is well documented that corals use the monthly cycle of moonlight to synchronize mass spawning events (Abe 1937; Harrison et al. 1984; Jokiel et al. 1985).

The monthly oscillation of moonlight may also cue synchronized dissepiment formation. Rotmann and Thomas (2012) showed that tissue layer thickness in *Porites* increases steadily throughout the lunar month before decreasing by 20% the day after the full moon. Combining this observation with our lunar rhythm results, we suggest the following mechanism of monthly growth cycles (Fig. 5). Through each lunar month, *Porites* polyps extend their skeletons and stretch their tissue layer, reaching maximum tissue thickness at the end of the lunar month. The full moon then cues the base of the tissue layer to uplift—decreasing the tissue thickness but not volume—and form a new dissepiment to rest on for the next lunar month (Fig. 5). Dissepiment spacing is thus a proxy for the monthly skeletal extension rate because the base of the tissue layer must keep pace with the top of the skeleton, at least over several months and in lieu of substantial changes in tissue layer thickness (Barnes and Lough 1993).



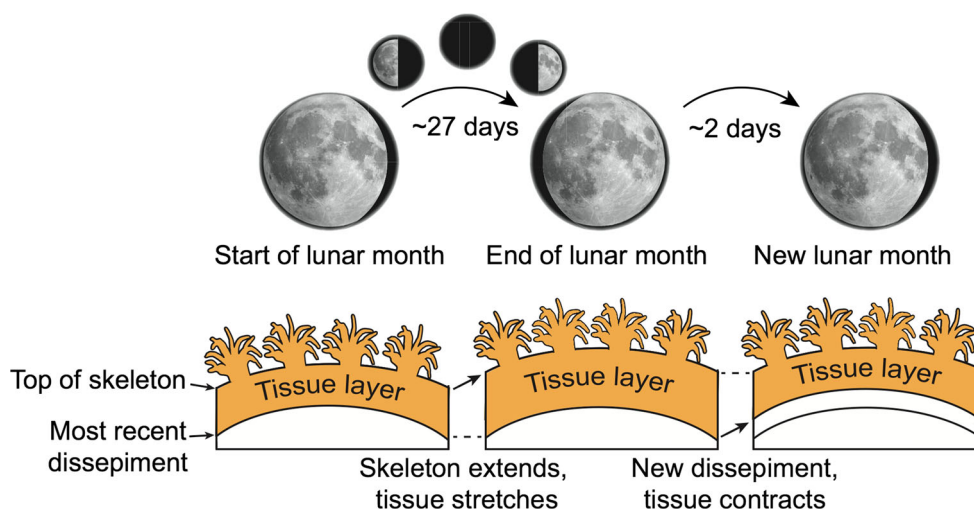


**Fig. 5** Schematic illustrating lunar rhythm of dissepiment formation. The living tissue layer rests on the most recently formed dissepiment. Over the course of the lunar month, the polyps extend the skeleton outward and the tissue layer thickness increases, reaching a maximum at the end of the lunar month (Rotmann and Thomas 2012). Within 1–2 d after the full moon, a new dissepiment is formed, the tissue

contracts or uplifts, and the previous dissepiment is preserved in the skeleton below. Without changes in tissue layer thickness over the year, the spacing between two consecutive dissepiments must be approximately equal to the extension at the top of the colony over the previous lunar month

The results of our study support the idea that dissepiments are lunar and thus can be used as a tool to construct high-resolution age models of coral skeletal growth or refine age models in seasonally resolved paleorecords. Dissepiments may be applied to improve annually resolved age models and growth histories to monthly resolution, to confirm density-based age models where some ambiguity exists in the banding pattern, and potentially even to develop age models for corals that lack clear annual density bands altogether.

### The mechanism of density band formation

The lunar rhythm of dissepiments makes them passive tracers of monthly variations in colony extension. Here, we use dissepiments as a tool to investigate how skeletal density banding is linked to changes in monthly growth rates.

Annual density bands in coral skeletons were discovered in X-radiographs decades ago (Knutson et al. 1972; Bud-demeier 1974; Dodge and Vaisnys 1975), yet mechanisms underlying growth-band formation have not been unambiguously identified (Helmle and Dodge 2011). Models of coral growth imply that density banding could arise from seasonal variations in the rate of skeletal thickening within the tissue layer, or from seasonal variations in thickening and extension rates (Taylor et al. 1993). Regular cycles of dissepiment spacing (i.e., monthly skeletal extension rate) have been observed in some cases (Barnes and Lough 1989) but were not linked to density-banding patterns (Barnes and Lough 1993). In our analyses, we found a clear

connection between dissepiment spacing and density banding in two corals from Palmyra Atoll (Fig. 6). Palmyra colony 03 has cycles of dissepiment spacing coherent with density bands, but Palmyra colony 02 has neither dissepiment spacing cycles nor density bands. These data suggest that annual density bands are produced if the tissue layer extends and uplifts, at different rates over the course of a year. When extension is relatively fast, the actively calcifying surface of the colony resides in a particular band for relatively little time. This produces relatively thin skeletal elements and low bulk density because the  $\text{CaCO}_3$  is accreted over relatively more volume, and vice versa for high-density bands (Fig. 6).

Taylor et al. (1993) modeled annual density banding in *Porites* with three growth processes: extension, skeletal thickening within the tissue layer, and monthly tissue uplift (i.e., dissepiment formation). We followed a similar approach to reproduce the Palmyra colony 03 density profile based on our dissepiment measurements. However, without measurements of the rate of skeletal thickening within the tissue layer, we held this variable constant. Using only the annual calcification rate and our dissepiment spacing time series, and assuming that monthly extension is equal to dissepiment spacing, we were able to reproduce several aspects of the measured density profile (Fig. 7). The timing and amplitude of annual density oscillations are similar between the model and the measurements, implying that seasonal variations in dissepiment spacing alone can produce annual density bands. Nevertheless, Taylor et al. (1993) found an important role for skeletal thickening in their modeling study, and variations



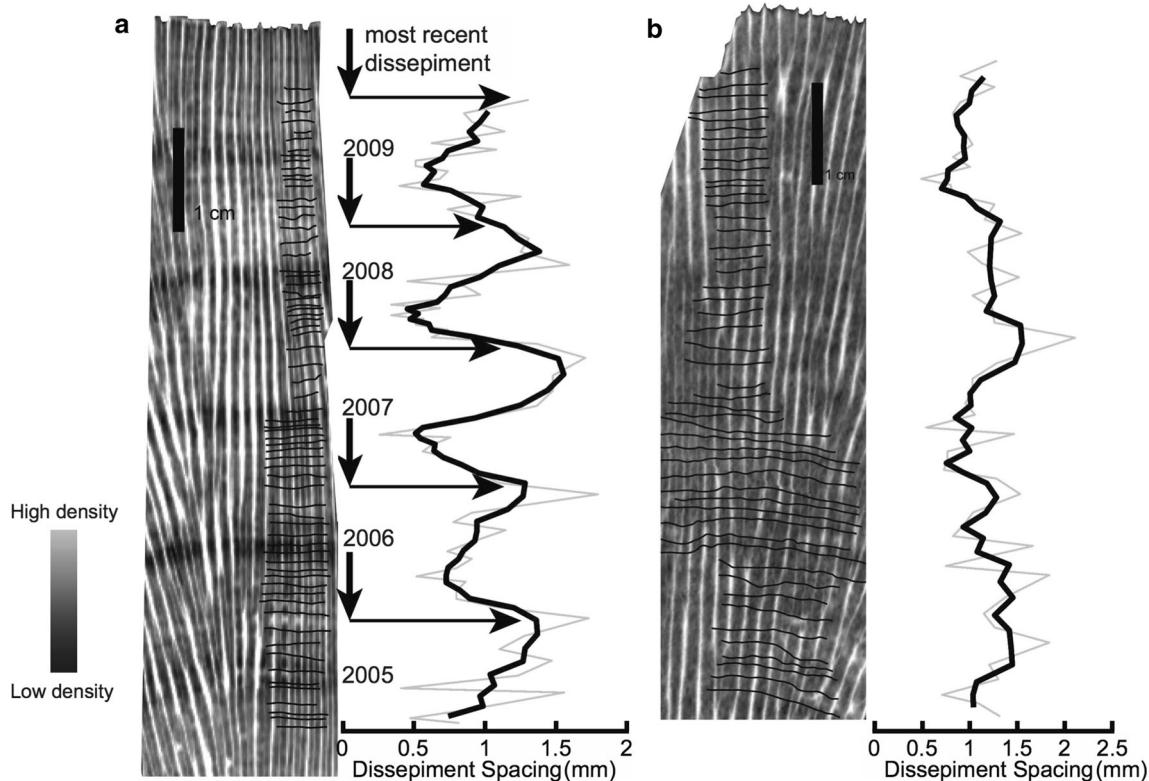


**Fig. 6** Dissepiments (*black lines*) traced on CT scan images of colonies Palmyra 03 (**a**) and Palmyra 02 (**b**), in which light/dark shading indicates relatively high/low-density skeleton. The plot to the right of each CT scan shows the spacing between successive dissepiments (*gray*) and 3-month moving average (*black*). For the

Palmyra 03 colony, we assumed that the tissue layer thickness is constant in time, and thus the density-banding pattern corresponds to dissepiment spacing further down-core (*black arrows*) at a distance equal to the tissue thickness (7 mm in this case). This shows that low-density bands are associated with peak dissepiment spacing

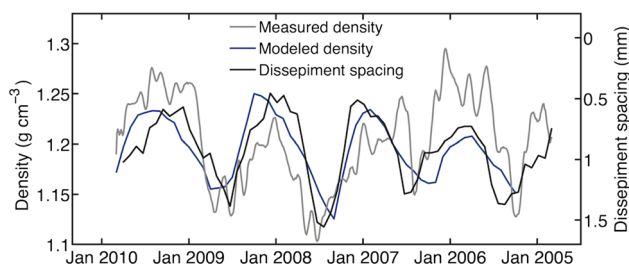


**Fig. 7** Modeled (*blue*) and measured (*gray*) skeletal density, and dissepiment spacing (*black*) plotted against time in the Palmyra 03 colony. Note that the y-axis scale is reversed for dissepiment spacing

in the rate of thickening could explain the subtle differences between our measured density profile and that modeled with only our dissepiment measurements (Fig. 7).

The mechanisms of density banding may also vary among species or genera. For example, Dodge et al. (1993) found no link between dissepiment spacing and density banding in the Caribbean coral *Orbicella annularis*. In *Orbicella* and other imperforate genera, the septa and thecal walls enclose each polyp, and there are two types of dissepiments: endothecal dissepiments at the bottom of the calyx and exothecal dissepiments between neighboring

polyps (Veron 1986). Dodge et al. (1993) suggested that variations in the thickness of exothecal dissepiments cause density banding in *O. annularis*. In contrast, the dissepiments in *Porites* are too small to substantially affect the bulk skeletal density, and because it is a perforate genus it does not have exothecal dissepiments (Barnes and Lough 1993). Thus, our findings may be specific to *Porites*, and potentially other perforate genera including *Pavona* and *Acropora* (Barnes and Lough 1993; van Woesik et al. 2013), but may not extend to imperforate genera such as *Orbicella*.

### High-density stress banding

Perturbations to the regular annual oscillation of skeletal extension reveal the sensitivity of corals to anomalies in the environment in which they live. Several studies have retroactively identified past coral bleaching events based on the presence of anomalous high-density bands in the skeletons of long-lived colonies (Carilli et al. 2009a, b; Cantin and Lough 2014; Mallela et al. 2015; Barkley and Cohen 2016). Suzuki et al. (2003) suggested that stress bands are produced during growth hiatuses, but this

hypothesis has not yet been tested using dissepiments. We produced a 9-yr time series of dissepiment spacing in a coral core from Airai Bay in the Republic of Palau that contains a prominent stress band in 1998, when unusually warm waters caused mass coral bleaching around the Palauan archipelago (Bruno et al. 2001; Barkley and Cohen 2016). Within the stress band, skeletal extension decreased sharply and only ten dissepiments are present between the 1998 and 1999 low-density bands (Fig. 8). Thus, stress bands may represent extreme versions of annual high-density bands in which extension not only slows, but ceases temporarily. Corals continue to calcify during bleaching, albeit at reduced rates (Fig. 8d, e), but without upward extension, they accrete a distinct high-density band. In our core, extension apparently ceased for 2–3 months, but this duration could vary among different thermal stress events or colonies (e.g., Suzuki et al. 2003 report a 4- to 5-month growth hiatus during bleaching).

The mechanism of stress-band formation is further evident in the geochemistry of the skeleton. Corals accrete their skeletons from an extracellular calcifying fluid located between the living tissue and the skeleton (Barnes

1970; Venn et al. 2011). By actively modifying the carbonate chemistry of this fluid—specifically, by elevating carbonate ion concentration ( $[\text{CO}_3^{2-}]$ )—corals rapidly nucleate and grow the aragonite ( $\text{CaCO}_3$ ) crystals that compose their skeletons (Cohen and Holcomb 2009; Venn et al. 2011; Cai et al. 2016). Variations in calcifying fluid  $[\text{CO}_3^{2-}]$  are recorded by the uranium-to-calcium ratio (U/Ca) in the skeleton because uranyl carbonate complexes are incorporated into the aragonite crystals in inverse proportion to  $[\text{CO}_3^{2-}]$  (Swart and Hubbard 1982; DeCarlo et al. 2015a). Across the stress band of the Airai coral, U/Ca spikes to higher values, indicative of reduced calcifying fluid  $[\text{CO}_3^{2-}]$  during bleaching (Fig. 8). This pattern was reproduced in another coral from Nikko Bay that also contains a prominent 1998 stress band (ESM Fig. S12). Schoepf et al. (2014) also investigated the sensitivity of U/Ca to bleaching, using *Porites divaricata* and *P. astreoides* in a 6-week experiment. They found that bleaching reduced calcification rates and increased U/Ca (i.e., reduced calcifying fluid  $[\text{CO}_3^{2-}]$ ) in *P. astreoides*, but not in *P. divaricata*. Bleached corals catabolize their own tissues to compensate for the energy production lost along

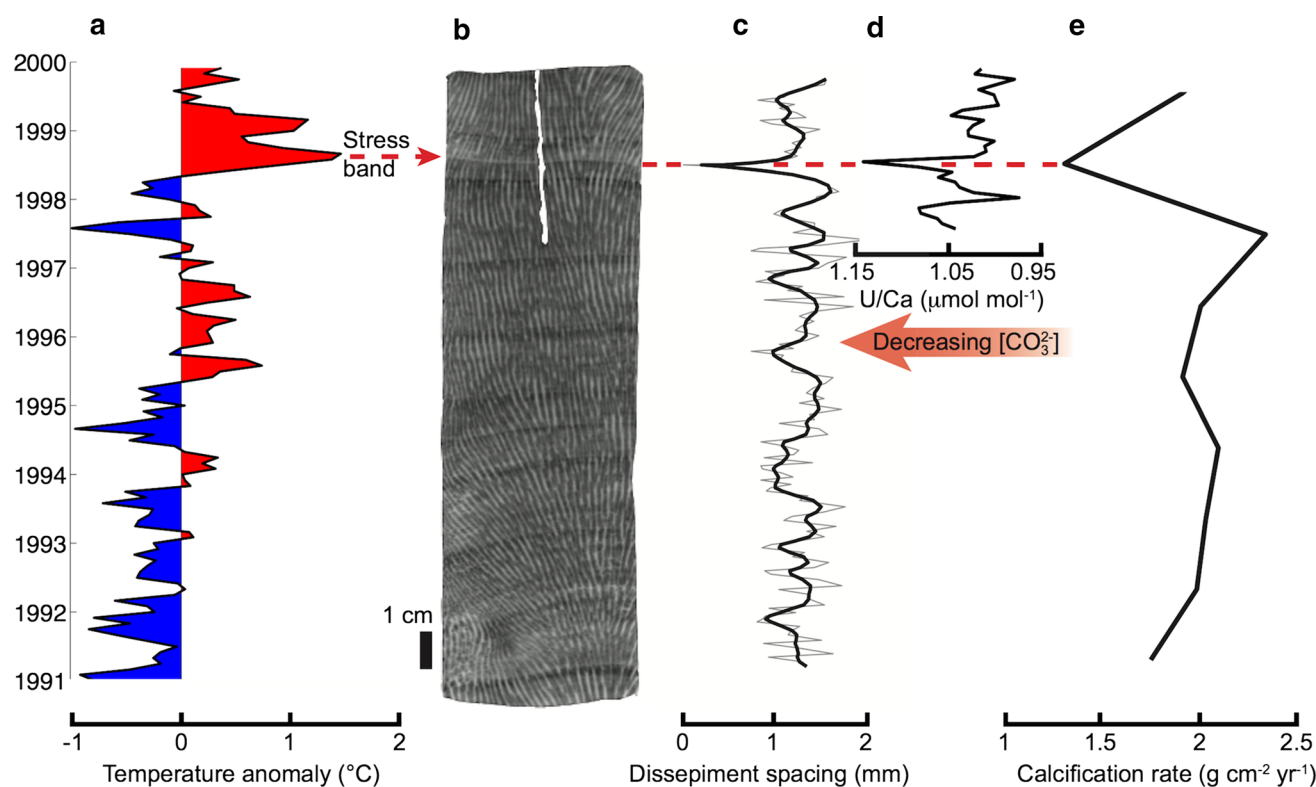


**Fig. 8** **a** Monthly temperature anomalies in the  $1^\circ$  grid-box surrounding Palau, derived from the NOAA Optimal Interpolation product (Reynolds et al. 2002) and calculated relative to the 1991–1999 monthly means. Unusually warm temperatures are plotted in red and unusually cool temperatures in blue. **b** The 1998 stress band in the CT scan of the Airai coral (red dashed line) The stress

band corresponds to **c** low dissepiment spacing, **d** high U/Ca ratios (i.e., low calcifying fluid  $[\text{CO}_3^{2-}]$ ), and **e** low annual calcification rate. The thin gray line in (c) is monthly dissepiment spacing, and the thick black line is 3-month low-pass filtered dissepiment spacing. The gap in skeleton at the top of this core was drilled for U/Ca analyses, and the U/Ca data were originally reported in DeCarlo et al. (2016)

with their symbionts (Mendes and Woodley 2002), and the geochemical signature of bleaching may only appear once the coral's energetic reserves have been depleted beyond a certain threshold (Schoepf et al. 2014). The species-specific responses in the experiments of Schoepf et al. (2014) potentially reflect differences in energetic reserves or energy allocated to calcification. Consistent between our results and those of Schoepf et al. (2014) though, is that U/Ca increases in the skeletons of *Porites* colonies whose calcification rates decrease during bleaching, implying that the impact of bleaching on calcification is via reduced calcifying fluid [ $\text{CO}_3^{2-}$ ]. Our dissepiment spacing and U/Ca data are thus consistent with hypotheses that corals' symbionts stimulate calcification (Goreau and Goreau 1959; Cohen and Holcomb 2009) and influence the geochemistry of the skeleton (Cohen et al. 2002), and they support the application of high-density "stress bands" as proxies of past bleaching events that last for at least 2–3 months.

The results of our study show that density banding in *Porites* coral skeleton arises from sub-annual variations in extension rate. These variations control the amount of time that the actively calcifying colony surface resides in a particular band, leading to a spectrum of skeletal density patterns. Annual density bands are a result of this process, as are distinct high-density "stress bands" (Figs. 6, 7, 8). Extension rate variability, and thus the resulting density-banding pattern, is likely driven by a combination of environmental and genetic factors. Coral calcification is sensitive to both temperature and light (Helmlle and Dodge 2011), yet *Porites* colonies that grew directly adjacent to one another and experienced the same conditions can have very different banding patterns (Fig. 6). This suggests that phenotypic variability among colonies or species may play a role. Temperature and light do not directly affect the density of  $\text{CaCO}_3$  deposited, but rather influence the coral animal, its zooxanthellae algae, or the symbiosis between the two. Ultimately, skeletal banding patterns reflect the sensitivity of the coral holobiont to environmental variability, but these sensitivities—and the environmental forcing involved—may vary among reef locations, species, phenotypes, and potentially even over time.

**Acknowledgements** We thank Yimnang Golbuu (Palau International Coral Reef Center) for assistance with permits and hosting us at PICRC, Hannah Barkley, G.P. Lohmann, Chip Young, and Kathryn Pietro for help with fieldwork, Burnham Petrographics for mounting and polishing sections, and Horst Marschall for assistance with microscope analyses. We thank two anonymous reviewers for their helpful comments. This work was supported by NSF Grants OCE 1220529 and OCE 1605365 awarded to A.L. Cohen, a WHOI Ocean Ventures Fund award to T.M. DeCarlo, a WHOI Coastal Ocean Institute award to T.M. DeCarlo, and an NSF Graduate Research Fellowship to T.M. DeCarlo.

## References

- Abe N (1937) Postlarval development of the coral *Fungia actiniformis* var. palawensis Doderlein. Palao Tropical Biological Station Studies 1:73–93
- Barkley HC, Cohen AL (2016) Skeletal records of community-level bleaching in *Porites* corals from Palau. Coral Reefs 35:1407–1417
- Barkley HC, Cohen AL, Golbuu Y, Starczak VR, DeCarlo TM, Shamberger KE (2015) Changes in coral reef communities across a natural gradient in seawater pH. Sci Adv 1:e1500328
- Barnes DJ (1970) Coral skeletons: an explanation of their growth and structure. Science 170:1305–1308
- Barnes DJ, Lough JM (1989) The nature of skeletal density banding in scleractinian corals: fine banding and seasonal patterns. J Exp Mar Bio Ecol 126:119–134
- Barnes DJ, Lough JM (1992) Systematic variations in the depth of skeleton occupied by coral tissue in massive colonies of *Porites* from the Great Barrier Reef. J Exp Mar Bio Ecol 159:113–128
- Barnes DJ, Lough JM (1993) On the nature and causes of density banding in massive coral skeletons. J Exp Mar Bio Ecol 167:91–108
- Bruno J, Siddon C, Witman J, Colin P, Toscano M (2001) El Niño-related coral bleaching in Palau, western Caroline Islands. Coral Reefs 20:127–136
- Buddemeier RW (1974) Environmental controls over annual and lunar monthly cycles in hermatypic coral calcification. Proc 2nd Int Coral Reef Symp 2:259–267
- Buddemeier RW, Kinzie RA (1975) The chronometric reliability of contemporary corals. In: Rosenberg G, Runcorn S (eds) Growth rhythms and the history of the earth's rotation. Wiley, London, pp 135–147
- Buddemeier RW, Maragos JE, Knutson DW (1974) Radiographic studies of reef coral exoskeletons: rates and patterns of coral growth. J Exp Mar Bio Ecol 14:179–199
- Cai W-J, Ma Y, Hopkinson BM, Grottoli AG, Warner ME, Ding Q, Hu X, Yuan X, Schoepf V, Xu H, Han C, Melman T, Hoadley KD, Pettay DT, Matsui Y, Baumann JH, Levas S, Ying Y, Wang Y (2016) Microelectrode characterization of coral daytime interior pH and carbonate chemistry. Nat Commun 7:11144
- Cantin NE, Lough JM (2014) Surviving coral bleaching events: *Porites* growth anomalies on the Great Barrier Reef. PLoS One 9:e88720
- Cantin NE, Cohen AL, Karnauskas KB, Tarrant AM, McCorkle DC (2010) Ocean warming slows coral growth in the central Red Sea. Science 329:322–325
- Carilli JE, Norris RD, Black B, Walsh SM, McField M (2009a) Century-scale records of coral growth rates indicate that local stressors reduce coral thermal tolerance threshold. Glob Chang Biol 16:1247–1257
- Carilli JE, Norris RD, Black BA, Walsh SM, McField M (2009b) Local stressors reduce coral resilience to bleaching. PLoS One 4:e6324
- Castillo KD, Ries JB, Weiss JM, Lima FP (2012) Decline of forereef corals in response to recent warming linked to history of thermal exposure. Nat Clim Chang 2:756–760
- Cobb KM, Charles CD, Cheng H, Edwards RL (2003) El Niño/Southern oscillation and tropical Pacific climate during the last millennium. Nature 424:271–276
- Cohen AL, McConnaughey TA (2003) Geochemical perspectives on coral mineralization. Reviews in Mineralogy and Geochemistry 54:151–187
- Cohen AL, Holcomb M (2009) Why corals care about ocean acidification: uncovering the mechanism. Oceanography 22:118–127



- Cohen AL, Layne GD, Hart SR, Lobel PS (2001) Kinetic control of skeletal Sr/Ca in a symbiotic coral: implications for the paleotemperature proxy. *Paleoceanography* 16:20–26
- Cohen AL, Owens KE, Layne GD, Shimizu N (2002) The effect of algal symbionts on the accuracy of Sr/Ca paleotemperatures from coral. *Science* 296:331–333
- DeCarlo TM, Cohen AL (2016) coralCT: software tool to analyze computed tomography (CT) scans of coral skeletal cores for calcification and bioerosion rates. *Zenodo*. doi:10.5281/zenodo.57855
- DeCarlo TM, Gaetani GA, Holcomb M, Cohen AL (2015a) Experimental determination of factors controlling U/Ca of aragonite precipitated from seawater: implications for interpreting coral skeleton. *Geochim Cosmochim Acta* 162:151–165
- DeCarlo TM, Gaetani GA, Cohen AL, Foster GL, Alpert AE, Stewart J (2016) Coral Sr–U thermometry. *Paleoceanography* 31:626–638
- DeCarlo TM, Cohen AL, Barkley HC, Cobban Q, Young C, Shamberger KE, Brainard RE, Golbuu Y (2015b) Coral macro-bioerosion is accelerated by ocean acidification and nutrients. *Geology* 43:7–10
- Dodge RE, Vaisnys JR (1975) Hermatypic coral growth banding as environmental recorder. *Nature* 258:706–708
- Dodge RE, Szmant AM, Garcia R, Swart PK, Forester A, Leder JJ (1993) Skeletal structural basis of density banding in the reef coral *Montastrea annularis*. In: *Proc 7th Int Coral Reef Symp* 1: 186–195
- Gladfelter EG (1983) Skeletal development in *Acropora cervicornis*: II. Diel patterns of calcium carbonate accretion. *Coral Reefs* 2:91–100
- Gorbanov MY, Falkowski PG (2002) Photoreceptors in the cnidarian hosts allow symbiotic corals to sense blue moonlight. *Limnol Oceanogr* 47:309–315
- Goreau TF, Goreau NI (1959) The physiology of skeleton formation in corals. II. Calcium deposition by hermatypic corals under various conditions in the reef. *Biol Bull* 117:239–250
- Harrison PL, Babcock RC, Bull GD, Oliver JK, Wallace CC, Willis BL (1984) Mass spawning in tropical reef corals. *Science* 223:1186–1189
- Helmle K, Dodge R (2011) Sclerochronology. In: Hopley D (ed) *Encyclopedia of modern coral reefs*. Springer, Netherlands, pp 958–966
- Highsmith RC (1979) Coral growth rates and environmental control of density banding. *J Exp Mar Bio Ecol* 37:105–125
- Hoegh-Guldberg O, Mumby PJ, Hooten AJ, Steeneck RS, Greenfield P, Gomez E, Harvell CD, Sale PF, Edwards AJ, Caldeira K, Knowlton N, Eakin CM, Iglesias-Prieto R, Muthiga N, Bradbury RH, Dubi A, Hatzitolos ME (2007) Coral reefs under rapid climate change and ocean acidification. *Science* 318:1737–1742
- Holcomb M, Cohen AL, McCorkle DC (2013) An evaluation of staining techniques for marking daily growth in scleractinian corals. *J Exp Mar Bio Ecol* 440:126–131
- Hudson JH (1981a) Response of *Montastrea annularis* to environmental change in the Florida Keys. *Proc 4th Int Coral Reef Symp* 2: 233–240
- Hudson JH (1981b) Growth rates in *Montastrea annularis*: a record of environmental change in Key Largo Coral Reef Marine Sanctuary, Florida. *Bull Mar Sci* 31:444–459
- Hudson JH, Shinn EA, Halley RB, Lidz B (1976) Sclerochronology: a tool for interpreting past environments. *Geology* 4:361–364
- Jokiel PL, Ito RY, Liu PM (1985) Night irradiance and synchronization of lunar release of planula larvae in the reef coral *Pocillopora damicornis*. *Mar Biol* 88:167–174
- Kaniewska P, Alon S, Karako-Lampert S, Hoegh-Guldberg O, Levy O (2015) Signaling cascades and the importance of moonlight in coral broadcast mass spawning. *eLife* 4:e09991
- Knutson DW, Buddemeier RW, Smith SV (1972) Coral chronometers: seasonal growth bands in reef corals. *Science* 177:270–272
- Lough JM, Barnes DJ (1990) Intra-annual timing of density band formation of *Porites* coral from the central Great Barrier Reef. *J Exp Mar Bio Ecol* 135:35–57
- Lough JM, Barnes DJ (1992) Comparisons of skeletal density variations in *Porites* from the central Great Barrier Reef. *J Exp Mar Bio Ecol* 155:1–25
- Mallela J, Hetzinger S, Halfar J (2015) Thermal stress markers in *Colpophyllia natans* provide an archive of site-specific bleaching events. *Coral Reefs* 35:181–186
- Mendes JM, Woodley JD (2002) Effect of the 1995–1996 bleaching event on polyp tissue depth, growth, reproduction and skeletal band formation in *Montastraea annularis*. *Mar Ecol Prog Ser* 235:93–102
- Reynolds RW, Rayner NA, Smith TM, Stokes DC, Wang W (2002) An improved in situ and satellite SST analysis for climate. *J Clim* 15:1609–1625
- Rotmann S, Thomas S (2012) Coral tissue thickness as a bio-indicator of mine-related turbidity stress on coral reefs at Lihir Island, Papua New Guinea. *Oceanography* 25:52–63
- Saenger C, Cohen AL, Oppo DW, Halley RB, Carilli JE (2009) Surface-temperature trends and variability in the low-latitude North Atlantic since 1552. *Nat Geosci* 2:492–495
- Schoepf V, McCulloch MT, Warner ME, Levas SJ, Matsui Y, Aschaffenburg MD, Grottoli AG (2014) Short-term coral bleaching is not recorded by skeletal boron isotopes. *PLoS One* 9:e112011
- Shamberger KE, Cohen AL, Golbuu Y, McCorkle DC, Lentz SJ, Barkley HC (2014) Diverse coral communities in naturally acidified waters of a Western Pacific reef. *Geophys Res Lett* 41:499–504
- Shirai K, Sowa K, Watanabe T, Sano Y, Nakamura T, Clode P (2012) Visualization of sub-daily skeletal growth patterns in massive *Porites* corals grown in Sr-enriched seawater. *J Struct Biol* 180:47–56
- Smith SV, Buddemeier RW, Redalje RC, Houck JE (1979) Strontium-calcium thermometry in coral skeletons. *Science* 204:404–407
- Smithers SG, Woodroffe CD (2001) Coral microatolls and 20th century sea level in the eastern Indian Ocean. *Earth Planet Sci Lett* 191:173–184
- Soong K, Chen C, Chang J-C (1999) A very large poritid colony at Green Island, Taiwan. *Coral Reefs* 18:42
- Sorauf J (1970) Microstructure and formation of dissepiments in the skeleton of the recent Scleractinia (hexacorals). *Biomaterialization* 2:1–22
- Suzuki A, Gagnon MK, Fabricius K, Isdale PJ, Yukino I, Kawahata H (2003) Skeletal isotope microprofiles of growth perturbations in *Porites* corals during the 1997–1998 mass bleaching event. *Coral Reefs* 22:357–369
- Swart PK, Hubbard JAEB (1982) Uranium in scleractinian coral skeletons. *Coral Reefs* 1:13–19
- Sweeney AM, Boch CA, Johnsen S, Morse DE (2011) Twilight spectral dynamics and the coral reef invertebrate spawning response. *J Exp Biol* 214:770–777
- Taylor RB, Barnes DJ, Lough JM (1993) Simple models of density band formation in massive corals. *J Exp Mar Bio Ecol* 167:109–125
- Thompson WG, Spiegelman MW, Goldstein SL, Speed RC (2003) An open-system model for U-series age determinations of fossil corals. *Earth Planet Sci Lett* 210:365–381
- van Woesik R, van Woesik K, van Woesik L, van Woesik S (2013) Effects of ocean acidification on the dissolution rates of reef-coral skeletons. *PeerJ* 1:e208

- Venn A, Tambutté E, Holcomb M, Allemand D, Tambutté S (2011) Live tissue imaging shows reef corals elevate pH under their calcifying tissue relative to seawater. *PLoS One* 6:e20013
- Veron JEN (1986) *Corals of Australia and the Indo-Pacific*. Angus & Robertson, Sydney, Australia
- Weber JN, Woodhead PMJ (1972) Temperature dependence of oxygen-18 concentration in reef coral carbonates. *J Geophys Res* 77:463–473
- Wells JW (1963) Coral growth and geochronometry. *Nature* 197:948–950
- Winter A, Sammarco PW (2010) Lunar banding in the scleractinian coral *Montastraea faveolata*: fine-scale structure and influence of temperature. *J Geophys Res* 115:G04007